Performance of Direct Injected Propane and Gasoline in a High [1]Stroke-to-Bore ratio SI Engine: Pathways to Diesel Efficiency Parity with Ultra Low Soot

D. Splitter, V. Boronat, F. Chuahy, and J.Storey,

ORNL- Oak Ridge National Laboratory. 2360 Cherahala Blvd., 37932 TN, USA.

E-mail: splitterda@ornl.gov
Telephone: +(1) 865 341 1347

Abstract. This work explores pathways to achieve diesel-like, high-efficiency combustion with stoichiometric 3-way catalyst compatible combustion in a single-cylinder spark ignition (SI) research engine. A unique high stroke-to-bore engine design (1.5:1) with cooled exhaust gas recirculation (EGR) and high compression ratio (r_c) was used to improve engine efficiency by up to 30% compared with a production turbocharged gasoline direct injection spark ignition engine.

Engine experiments were conducted with both 91 RON E10 gasoline and liquified petroleum gas (LPG) (i.e., autogas) and were compared to legacy gasoline data on the production engine. Geometric compression ratio (**r_c**) of 13.3:1 was used for both fuels with additional experiments at 16.8:1 for LPG only. Measurements of exhaust soot particle size and number concentrations were made with both fuels. Significant reduction in soot particles across the whole particle size range were achieved with LPG due to the elimination of in-cylinder liquid films. The effects of EGR, late intake valve closing (IVC) and fuel characteristics were investigated through their effects on efficiency, combustion stability and soot production. Results of 47% gross thermal efficiency, and 45% net thermal efficiency at stoichiometric engine operation, at up to 17 bar IMEP and 2000 r/min with 16.8:1 r_c were achieved with LPG. Estimated brake efficiency values were compared to a contemporary medium duty diesel engine illustrating the benefits of the chosen path for achieving diesel efficiency parity.

1. Introduction

Achieving thermal efficiency parity with diesel engines is one of the major challenges of stoichiometric spark ignition (SI) engines, yet it is a promising path forward to reduce greenhouse gas emissions and simplify criteria pollution control through the use of three-way catalysts (TWC). Stoichiometric SI combustion presents major disadvantages when compared to diesel combustion. Primarily SI engine design is limited by knock, and thus r_c's of less than 12 are typical. Additionally, the need for a stoichiometric mixture for TWC operation eliminates the possibility of air dilution, a known strategy to improve combustion thermodynamic efficiency. Nevertheless, exhaust gas recirculation (EGR) can be used to mitigate this loss [1], while also reducing knock in naturally aspirated engines [2]. Mixture dilution in these engines is achieved with cooled EGR. Combustion stability, measured by cycle-to-cycle variations, limits the dilution level and thus the efficiency benefits that can be achieved. At high engine loads, cooled EGR becomes less effective at reducing knock and can even cause knock to increase [3]. At part load, SI engines require throttling to control the air fuel ratio of the mixture, introducing pumping losses. These losses can be reduced with flexible valve operating strategies like late intake valve closing [4], which can be provide additional benefits when combined

This manuscript has been authored by UT-Battelle, LLC, under Contract No. DE-AC0500OR22725 with the U.S. Department of Energy. The United States Government retains and the publisher, by accepting the article for publication, acknowledges that the United States Government retains a non-exclusive, paid-up, irrevocable, world-wide license to publish or reproduce the published form of this manuscript, or allow others to do so, for the United States Government purposes. The Department of Energy will provide public access to these results of federally sponsored research in accordance with the DOE Public Access Plan (http://energy.gov/downloads/doe-public-access-plan).

with cooled EGR [2]. Finally, SI engines are susceptible to stochastic pre-ignition (SPI) which can severely limit engine load and efficiency [5,6].

A major benefit of SI engines is that they allow the use of low carbon content fuels like methane and propane. Additionally, criteria pollutant control, like unburned hydrocarbons, carbon monoxide and nitrogen oxides (UHC, CO and NOx) is extremely efficient and does not require an additional reducer, as in selective catalytic reduction (SCR) systems, characteristic of diesel engines. Consequently, it is of interest to develop ways of closing the efficiency gap between diesel and stoichiometric SI engines combining the best characteristics of each system.

The control of criteria pollutants (UHC, CO and NOx) in stoichiometric SI engines has evolved quite substantially. Conversion efficiencies over a warm catalyst approaching 99.9% are common, reducing the challenge of emissions control to the first 30 seconds of a cold start. Additionally, precious metal loading in TWCs have been decreasing as thinner, lighter substrates with lower wash coat requirements are developed and thus substantially reduce aftertreatment cost [7,8].

At the same time, diesel engines are expected to meet significant technical barriers in being able to meet future NOx regulations. Recently the California air resources board (CARB) has announced its intention to reduce U.S. domestic NOx emission regulations for medium- and heavy-duty vehicles by an order of magnitude by 2027 [9]. While SCR systems are very effective at reducing NOx at steady state conditions, they require the use of urea as a reducer, which decreases the overall system fluid efficiency. Additionally, transient control requires complex control strategies to optimize urea consumption and formation of urea crystal deposits. The major challenge with upcoming MD/HD regulations is the requirement to maintain NOx control under extremely low engine loads. SCR systems currently cannot operate effectively below 170°C due to poor urea decomposition and low ammonia storage in the substrate. Currently, the deactivation of SCR systems at low temperatures is responsible for a large disparity between cycle-measured emissions during engine certification and real-world operation [10]. Current diesel NOx control research [11] which assesses the feasibility of meeting the proposed regulations showed that additional close-coupled catalysts and NOx traps may be required. These measures are expected to increase the cost of diesel aftertreatment system by as much as 100% [10]. The return on investment of the additional emissions control costs is duty-cycle dependent and may not be feasible for medium-duty vehicles with low annual mileage.

Currently, SI engines can achieve the criteria emissions regulation targets proposed for diesel engines by California Air Resource Board (CARB) [9,12]. However, due to their relatively low fuel efficiency, achieving phase 1 and phase 2 CO_2 emission regulations [13] is a challenge that is typically overcome by using fuels with higher hydrogen content (i.e., higher H/C ratio) than gasoline. While gasoline shows a marginal CO_2 improvement over diesel fuel for a given engine efficiency, liquefied petroleum gas (LPG) and compressed natural gas (CNG) can achieve significant reductions simply due to their lower carbon content. For engines with brake thermal efficiency (BTE) parity, LPG and CNG can reduce CO_2 emissions when compared to a diesel fuelled engine by 11.7% and 32.6%, respectively. Consequently, if an engine can achieve diesel-like efficiencies with LPG or CNG, there can be a simultaneous reduction in CO_2 emissions as well as a simplification, and cost reduction of the emissions control system. Both LPG and CNG exhibit high knock and pre-ignition resistance due to their high octane rating, which makes them great candidate fuels for high efficiency SI combustion. Their high volatility significantly reduce if not eliminate the formation of fuel films inside the cylinder during the injection process and likely results in reductions to soot and particulate matter emissions. Nevertheless, despite the potential advantages of both fuels, LPG offers significant advantages over CNG in terms of storage and delivery as it can be stored at relatively low pressures (~5 bar) and directly injected in common direct injection fuel systems with minor modifications. This makes it the more attractive choice for a simpler, cheaper system that could be rapidly adopted in the MD market. Consequently, the efficiency potential and particulate emissions of LPG in an SI direct injected (DI) engine will be a focus of the current work.

To achieve diesel-like efficiencies, loss mechanisms of stoichiometric SI engines must be identified and addressed. Additionally, technologies need to take advantage of the unique fuel properties to maximize engine performance. To that end, ORNL has recently commissioned a custom-built long stroke single-cylinder research engine (LSE) targeting high efficiency SI combustion, as first described in Boronat et al. [14]. To allow optimized control of mixture dilution, compression pressure and residual gases, the engine is fitted with EGR and a variable valve actuation system. The uniqueness of the platform comes in the form of a significantly larger stroke-to-bore ratio of 1.5:1 against a stock ratio of

1:1. The increase in stroke-to-bore ratio results in increased in cylinder turbulent kinetic energy (TKE), increasing turbulent flame speeds and reducing combustion durations. It is well documented that the use of “domed” pistons to achieve high compression ratio (r_c) is typically followed by increases in incomplete combustion due to flame quenching. The LSE avoids this limitation due to its increased piston travel distance and naturally higher geometrical r_c, thus further increasing the potential for efficiency improvements.

The present work builds on previously reported LSE results [14] and explores in detail the mechanisms by which the LSE can improve efficiency and what opportunities are left for further improvement. Results with both gasoline and propane (surrogate for LPG) are shown and contrasted in terms of performance and efficiency. Detailed soot measurements including filter smoke number, photoacoustic measurements and scanning mobility particle sizing (SMPS) are used to characterize the soot emissions of the engine with both fuels. Results are contrasted against legacy data on a similar engine platform, and assessments of LPG engine efficiency are made.

2. Experimental set up

2.1 Engine platform

The LSE is a custom platform based on the General Motors (GM) Ecotec LNF family of engines, and was developed to operate under a wide variety of modes and engine operating conditions.

The LSE was developed on custom-built billet block, crankshaft and connecting rods. Figure 1 shows pictures and a schematic of the LSE. Custom components were combined with a stock cylinder head and piston assemblies. The stock valve actuation system was replaced by a fully flexible Sturmann variable valve actuation (VVA) system. The system enables variation of valve lift, opening time and duration of actuation, with independent control of each valve. The ballistic response of the valves in the system does not allow it to mimic the stock valve lift profile and maximum valve lift is limited to 9mm (vs. stock of 10.2mm). Detailed discussion of this system on can be found in [15,16,17,18]. Computational fluid dynamic studies showed that for matched valve opening events minimal differences were observed on the flow pattern and TKE profile of the engine as repotted in Boronat et al. [14], thus allowing direct comparisons to be made between the LSE and the stock LNF.

The production LNF coil on plug assembly is retained and can deliver 80mJ of spark energy. A spark plug two heat ranges colder replaces the stock spark plug to avoid hot-spot-run-away events while exploring high load conditions. Table 1 shows a summary of the production engine and the LSE geometries. Naturally the longer stroke required a longer connecting rod, and results in a higher r_c for a given piston when compared to the stock engine.

Figure 1. LSE billet block, crankshaft and connecting rod. Cylinder head is equipped with a fully flexible valve actuation system by Sturman Industries. Engine was built for single cylinder operation. Custom crankshaft was built with two counterweights for overall engine balance.

Table 1. Stock LNF and LSE geometry information.

	LNF	LSE
Bore [mm]	86	86

Stroke [mm]	86	129
Connecting Rod [mm]	145	182.9
r_c [-]	9.2:1, 11.85, 13.8	13.3:1 (same piston as 9.2 LNF), 16.8 (same piston as 11.85 LNF)
Number of Valves	4	4
Displaced volume [l]	0.495	0.7493
Exhaust valve lift [mm]	10.2	9
Exhaust valve duration [°CA]	188	variable
Exhaust cam phasing authority [°CA]	-	variable
Inlet valve lift [mm]	10.2	9 (fixed in this study)
Intake valve duration [°CA]	200	variable
Intake cam phasing authority [°CA]	-	variable

Figure 2 shows the two piston geometries used in the experiments. The stock LNF piston results in a r_c of 9.2 on the stock engine. When used in the LSE r_c is increased to 13.3 for the same top-dead-center (TDC) volume. A second piston bowl was modified to achieve a higher r_c of 11.8:1 on the stock engine while avoiding a "domed" configuration. When installed in the LSE the r_c is increased to 16.8. Further details can be found on previous reported work [15]

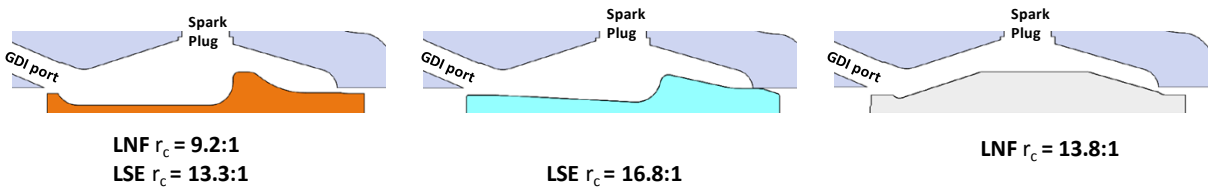

Figure 2. Piston geometries used in the present work with r_c noted for each design and respective engine below image.

2.2 Experimental Setup and Testing Methodology

Engine control was managed by a National Instruments control software combined with the Combustion Analysis Toolkit (DCAT) package. In cylinder pressure traces were measured using a piezo-electric pressure transducer made by Kistler (6125C). Engine crank position was acquired by a shaft mounted encoder (2614C11) providing a crank angle resolution of 0.2 crank angle degrees. For all experimental conditions 2000 consecutive combustion cycles were recorded to generate ensemble metrics. Engine air supply was managed by an Alicat 2000SLPM air mass controller. Air intake temperature was controlled using a Sylvania Suremax 800 heater placed upstream of the intake plenum. Intake and exhaust surge tanks were installed to mitigate pressure pulsations, characteristic of single cylinder engines, which could affect boundary condition measurements. A cooled EGR loop was installed between the intake and exhaust surge tanks. An EGR cooler was used to keep the gas outlet temperature at a constant 40°C. EGR was adjusted by an electronic actuated valve in the EGR system and an engine backpressure valve located downstream of the exhaust surge tank. Engine backpressure was adjusted to simulate a turbocharger with a combined efficiency of 40%, according to the calculation approach presented in [16].

Fuel supply was accomplished with six piston accumulators pressurized to 100 bar by nitrogen gas. Delivery pressure was finely controlled downstream of the accumulators by a TESCOM (ER3000SI-1) pneumatic pressure regulator. Fuel mass flow was measured by a Coriolis Micro-motion ELITE (CMF010P) flow meter. For all experimental conditions fuel injection timings were fixed at -280°CA aTDCf and spark timing was adjusted to achieve optimal thermodynamic efficiency while avoiding

knock. Peak cylinder pressure was limited to 100bar. Combustion stability as measured by the coefficient of variation (COV) of the indicated mean effective pressure (IMEP) was kept below 3%.

2.3 Emissions equipment

Exhaust was sampled for criteria pollutants (CO, CO2, HC, and NOx) through a sampling line heated to 190 °C downstream of the surge tank and analyzed with a number of instruments including non-dispersive infrared (NDIR) for CO and CO2 detection, flame ionization detection (FID) for THC measurements, and chemiluminescence detection (CLD) for NOx.

Particulate matter (PM) was characterized through particle size and number measurements and carbonaceous soot measurements. Carbonaceous soot was measured through a photoacoustic sensor (AVL microsoot). Figure 3 shows a schematic of the particle size distribution (PSD) measurement apparatus. An ejector pump-based microdilution system was used to sample the exhaust downstream of the surge tank. The ejector pump was mounted directly on the probe to minimize line lengths. Total dilution ratio was measured by the CO_2 ratio of samples before and after dilution using a Fourier transform infrared spectrometer (FTIR) and ranged from 10:1 to 12:1. A scanning mobility particle sizer (SMPS, TSI Model 3936) was used to measure the particle size distribution of the diluted sample. Combined with a differential mobility analyzer (DMA, TSI model 3081) and a condensation particle counter (CPC, TSI model 3025) particle sizes from 9.8 to 429nm and quantities were measured.

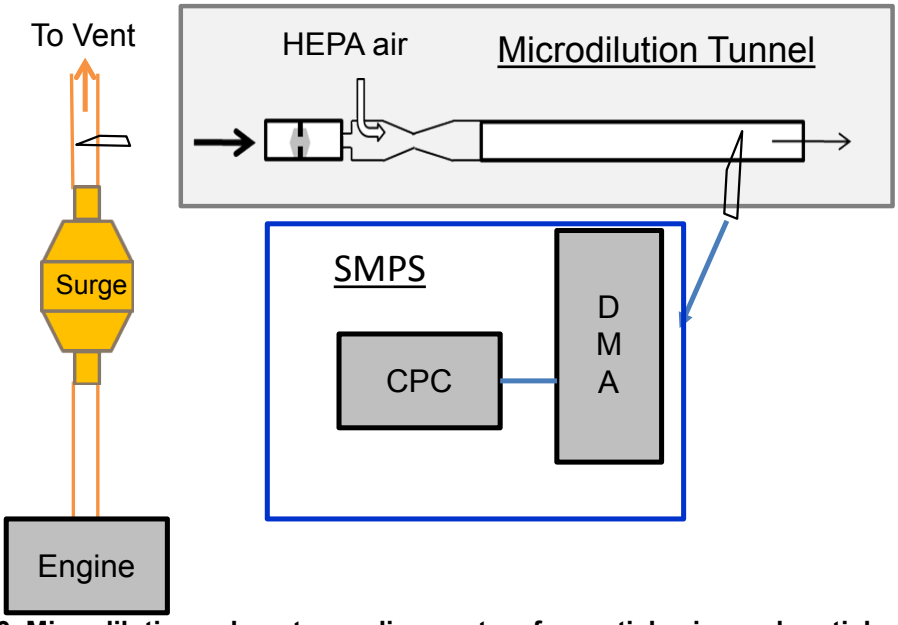

Figure 3. Microdilution exhaust sampling system for particle size and particle number quantification.

2.4 Fuels

The engine was operated with propane (~96% propane balanced with ~2% butane and ~2% ethylene), and an 87 anti-knock index (AKI) gasoline with 10% ethanol by volume. Table 2 shows a summary of fuel properties and composition.

Table 2. Fuel properties

	87 AKI E0	87 AKI E10	LPG
RON (ASTM D2699)	90.2	90.9	112
MON (ASTM D2700)	83.9	83.4	97
S (RON – MON)	6.3	7.5	15
Boiling Point [°C]	N/A	N/A	-42
10% [°F] (ASTM D86)	97	52.3	N/A

50% [°F] (ASTM D86)	205	94.3	N/A
90% [°F] (ASTM D86)	316	325	
C wt% (ASTM 5391)	86.49	82.78	82.78
H wt% (ASTM 5391)	14.06	13.59	17.22
O wt% (ASTM 5599)	0	3.63	0
LHV [MJ/kg] (ASTM D240)	43.454	41.410	46.4
oxygenates % vol. (ASTM 5599)	0	9.87	0

2.5 Combustion analysis

Synchronous and asynchronous experimental data were processed by an in-house MATLAB based post-processing routine. Cylinder pressure traces were filtered using a zero-phase filter and combined with camshaft position feedback to calculate in-cylinder trapped mass on a cycle by cycle basis using the approach proposed by Cavina et al. [19]. Heat transfer losses were estimated using Woschni correlation [20] and crevice losses were calculated using the approach of Gatowski et al. [21]. Apparent heat release is calculated from filtered pressure traces and combined with heat transfer and crevice losses to derive total heat release. Engine TDC was adjusted using a magnetic proximity probe (AVL OT-Sensor 428) during motoring operation and TDC loss angle was adjusted based on the approach reported by Tunestål et al. [22].

3. Results

The results section will be divided into 4 sections spanning analysis of efficiency and particulate emissions.

3.1 LSE and fuel effects on combustion duration and combustion efficiency

Initial results of combustion duration and incomplete combustion are plotted for gasoline and LPG in Figure 4 A and B respectively. The results compare the LSE to the production LNF engine. Note that the gasoline LNF data in Figure 4 A was originally reported in Splitter et al. [16,17,18], which used the same valve timings, piston, and Sturman cylinder head as in the present work. The gasoline results in Figure 4 A clearly highlight the advantages of the LSE platform with gasoline in a near r_c neutral analysis. Specifically, for a r_c of ~13.5:1 the LSE enables HC emissions equal to the production LNF engine (9.2 r_c) and thus reduced incomplete combustion losses. The source of these is attributed to the “dome” piston (Figure 2) needed in the LNF geometry to generate increased r_c. Clearly, the increased squish area in the dome design reduced combustion efficiency and increased combustion duration, effects that are well documented in the literature [23]. However, the approach used in the LSE offers high compression without increased quench and thus shows no effect to combustion efficiency; in fact combustion efficiency was seen to have increased with the LSE design, an effect attributed to increased charge motion. The increase in charge motion and reduction of quenching regions are evident on the combustion durations in Figure 4 A, where relative to the stock LNF, the dome piston showed increased combustion duration and the LSE showed reduced combustion duration. Note, that the increased r_c achieved through either the dome piston in the LNF or the stock piston in the LSE, result in earlier onset and more extreme knock, where the knock limited spark phasing effects on increasing combustion duration are also evident in the figure. Moreover, the similar r_c’s in the dome piston and stock piston in the LSE result in the knock limit near the same load.

Interestingly when the fuel is changed from gasoline to LPG as shown in Figure 4 B, the trends in combustion duration of the LSE and dome piston continue, but the effects of quench on combustion efficiency are much less clear. For all r_c’s and engine configurations tested it was observed that relative to gasoline, LPG offers improved combustion efficiency and reduced HC emissions. These effects are attributed to improved fuel vaporization from LPG compared to gasoline, and thus in-cylinder processes such as fuel films and injection strategy effects on mixing could be less pronounced with LPG than with gasoline. Interestingly the LSE still retains faster combustion than the

LNF, and for a given engine configuration there is no appreciable combustion duration difference between LPG and gasoline (LNF 9.2 r_c). Note that with LPG there was virtually no knock onset observed in either engine at the tested conditions and combustion phasing was retarded only because of peak cylinder pressure limits being reached.

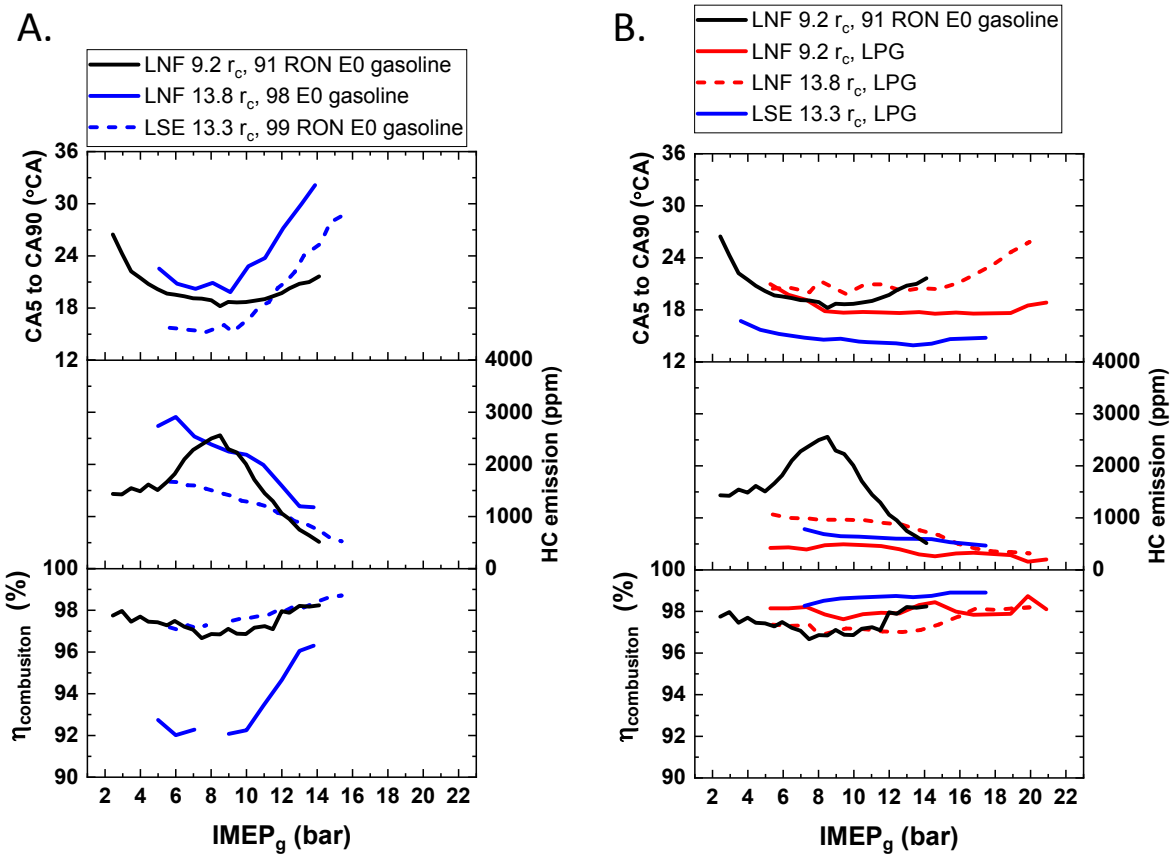

Figure 4 Combustion efficiency, HC emissions, and combustion duration for (A.) Gasoline only with LNF at r_c=9.2 and r_c=13.8:1 ratios and LSE at r_c=13.3:1, and (B) LPG and gasoline reference with LNF at r_c=9.2 and propane with LNF with r_c=13.8:1 ratios and LSE with r_c=13.3:

3.2 Long Stroke Engine Liquified Petroleum Gas Exhaust Gas Recirculation effects

The results in the previous section highlighted the combustion efficiency benefits that LPG offers over gasoline. Beyond these benefits, LPG also showed significantly improved EGR tolerance when compared to gasoline. Figure 5 shows that for all load conditions the COV of IMEP of LPG was overall lower than gasoline's and allowed a higher percentage of EGR before the COV limit was reached.

It is hypothesized that two main effects are responsible for the improved EGR tolerance performance of LPG; (1) Its laminar flame characteristics and (2) its flame stretch properties like Markstein length/number. As illustrated in the Borghi-Peters diagram [24] an increase in the laminar flame speed or reduction in the flame thickness of the fuel relative to turbulent velocity and length scales leads to a flame that is less prone to influences from the flow field. Flow field distortions of the flame kernel are believed to be one of the main components of cycle-to-cycle variation in spark ignition engines [25,26]. As EGR dilution is increased, the laminar flame speed of the fuel is reduced, and its flame thickness is increased. An increase in flame thickness makes the fuel more prone to influences from the flow field as turbulent eddies can corrugate the flame to a larger extent. LPG shows a lower thickening of the flame when EGR dilution is introduced, thus favoring its resistance to corrugation by turbulent eddies. LPG also shows a higher laminar flame speed than gasoline which allows it to have faster flame kernel formation and propagation, increasing the Dahmkoler number of the flame [27].

The second effect that contributes to LPG's higher EGR tolerance is related to its flame stretch properties. The Markstein length modifies the laminar flame speed of the fuel due to preferential diffusion effects. Under the conditions relevant to internal combustion engines the Markstein length is positive and relatively small, of the order of 0.1-0.2mm [28,29]. It is currently unknown how much these effects contribute to LPG's superior dilution tolerance in a real engine environment. Nevertheless, the Markstein length of propane is positive (i.e., stretch effects reduce the laminar flame speed of the fuel) and is smaller than the Markstein length for iso-octane, a surrogate for gasoline. As such, based on the available literature, LPG should be less susceptible to stretch effects. The effect of flame stretch is expected to increase the differences in laminar flame speed between LPG and gasoline. Flame stretch and preferential diffusion effects on flame kernel formation and effects on COV of IMEP is a topic that needs to be further explored to understand if the benefits of LPG can be extended by optimizing charge motion and turbulence.

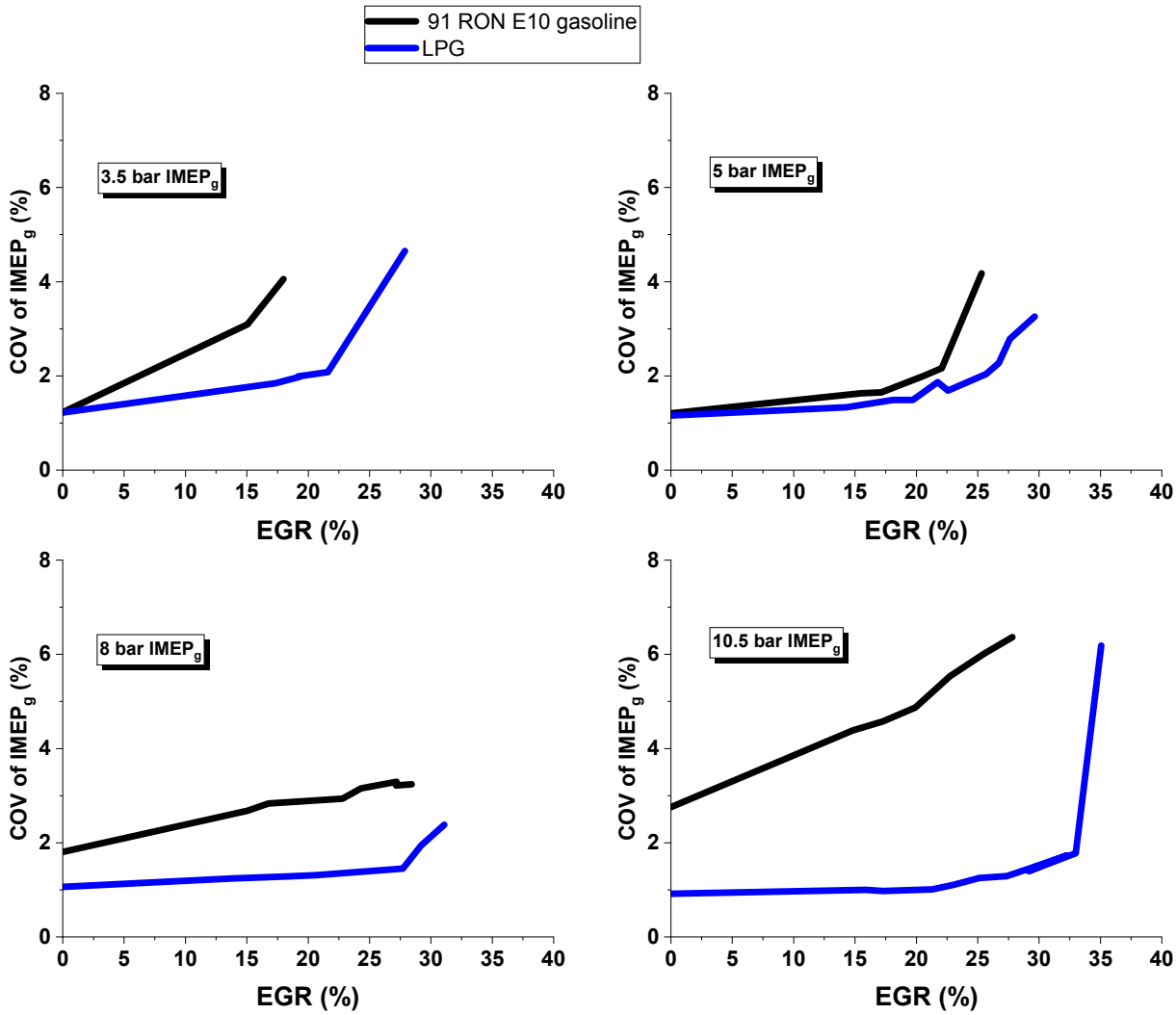

Figure 5. COV of IMEP for DI gasoline (black) and LPG (blue) for four loads as a function of EGR at 2000 r/min.

3.3 Long Stroke Engine Liquified Petroleum Gas operating strategies for increased efficiency

The combined effects of LPG on engine efficiency were explored in a systematic approach. The LNF engine was operated in its stock form with LPG, and with the 13.8 r_c piston ("dome" piston). These experiments were conducted with 0% EGR and conventional cam timings. Results of the LNF (and LSE) with LPG are presented in Figure 6. Relative to gasoline with no changes to the engine r_c or operating conditions, LPG extends the load range significantly, but offers no significant efficiency benefits (green vs black lines in Figure 6); however, if r_c is increased then LPG can increase efficiency

and simultaneously increase power density (blue vs black/green in Figure 6). At an 8 bar IMEP load, this results in approximately a 9.5% relative increase in efficiency compared to the baseline engine with either gasoline or LPG.

Using LPG but changing the engine from the LNF to the LSE offers further increase in efficiency observed (red vs green). These improvements are primarily due to reductions in heat transfer and combustion duration, as previously pointed out by Boronat et al. [14], there is also an increase in combustion efficiency which is minor but non-trivial. As shown in Figure 6, at an 8 bar IMEP load the LSE approach yields an approximate 16% relative improvement in efficiency compared to the baseline LNF. Although the LSE approach alone enabled good efficiency gain, the combination of EGR and even further increased r_c were also explored, which as shown in Figure 6, are where significant gains in efficiency can be realized. The high EGR rates possible with LPG were leveraged with late intake valve closing (110°CA bTDC vs 170°CA bTDC) and EGR. When used in tandem with 16.8 r_c this approach yielded nearly a 30% improvement in efficiency compared to the baseline LNF engine. Moreover, the power density of the LSE with LPG is not fully represented here due to the flowrate limit of the stock fuel injectors. With increased flow rate injectors higher power density should be achievable. It should be noted that the efficiency and power density of the LSE SI LPG engine approach those of current medium duty diesel engines.

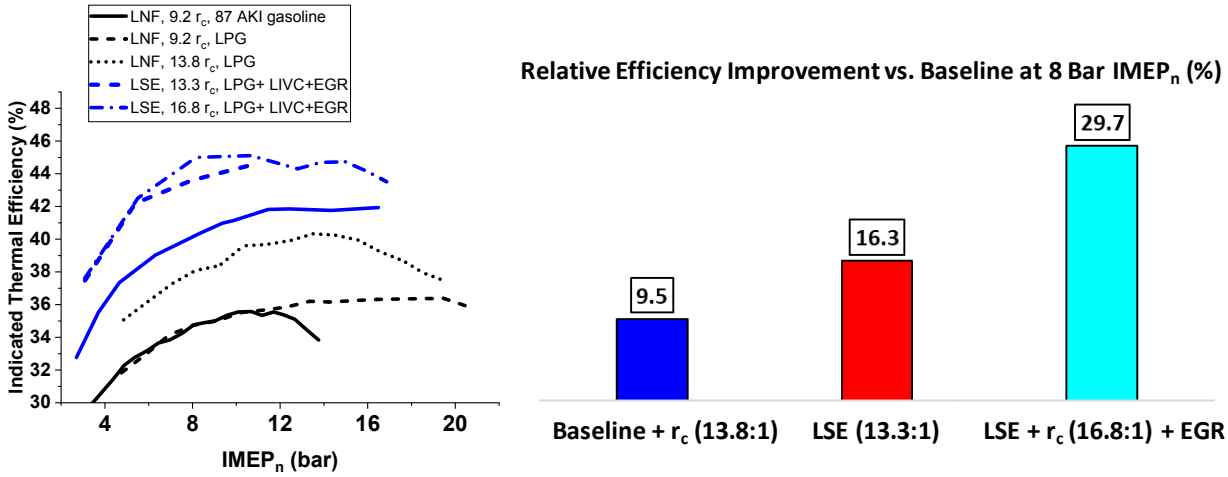

Figure 6. Efficiency improvement pathway for ORNL LSE engine with LPG, pathway combined EGR and high r_c

3.4 LPG and gasoline FSN, Soot, and Particle Size Distributions comparisons

The previous section highlighted that that stoichiometric LPG offered significant improvements in efficiency, EGR tolerance, and combustion efficiency compared to stoichiometric gasoline, achieving efficiencies similar to diesel engine results. To further assess stoichiometric LPG engine operation, this section explores differences between LPG and gasoline particulate emissions.

Engine operation over a wide load range and several EGR levels were conducted. The LSE engine was operated with only the production LNF piston installed (Figure 2). The filter smoke numbers (FSN) of EGR sweep at four loads spanning the range of low-to-high load are plotted in Figure 7. Note that the 10.5 bar IMEPg load for gasoline was heavily knock limited and near its maximum spark retard while LPG was just becoming knock limited at this condition, so at the highest loads the combustion phasings were not matched, but at lower loads they are. At each load EGR was swept from 0% to the maximum possible until unstable engine operation occurred. The loads and conditions are the same as those presented in Figure 5, where COV of IMEP beyond 3 is where unstable operation existed.

Results in Figure 7 clearly show that LPG exhibits extremely low FSN values, effectively zero FSN for all EGR rates and loads ranging from 3.5 bar IMEPg to 10.5 bar IMEPg. TI is well known that fuel volatility and subsequent fuel wall wetting can be correlated with FSN and particulate emissions in SI DI engines. Szybist et al. [30] conducted several studies with DI in a GM LNF engine (i.e., the same engine the LSE in the present work is based on) and found that increased volatility fuels, like E20 and E85, and multiple injection events could be used to reduce particle emissions. That work and other

simulation [31] and optical measurements [32], all support the hypothesis that the source of DI gasoline particulates is primarily form surface wetting.

These previous findings and the combined results further support the current hypothesis of reduced wall wetting with DI LPG compared to gasoline. The present results also show in Figure 7 that with LPG there is significantly reduced HC emissions, approximately 1/3 to 1/2 those of gasoline. These results are also observable with 0% EGR over a load sweep with several different engine configurations in Figure 4. The very low HC and effectively zero FSN with LPG regardless of load and EGR rate in Figure 7 combined with the similar findings regardless of engine configuration in Figure 4strongly suggest that DI LPG has very low surface wetting. Interestingly the results in Figure 7 also highlight that for gasoline, as EGR rate is increased FSN tends to be stable or decrease, with the latter prevalent at increased engine loads. Similar trends were also observed by Alger et al. [33] and Zhang et al. [34], where the latter work pointed out that as EGR rates increased the particle accumulation mode decreased and particles were primarily accumulation mode independent of fuel type used. In the present work similar processes appear to be occurring in gasoline, but at least for FSN there seems to be no appreciable FSN from LPG entirely. Previous works attributed the accumulation mode to HC emissions; however, the present work observed an increase in HC emission in both gasoline and LPG with increased EGR rates, however, unlike gasoline, increased HC emission with LPG did not observe an increase in FSN. This suggests that with LPG, soot formation pathways from HC could eb different. To further explore the particles of LPG and gasoline further measurements and analysis were conducted.

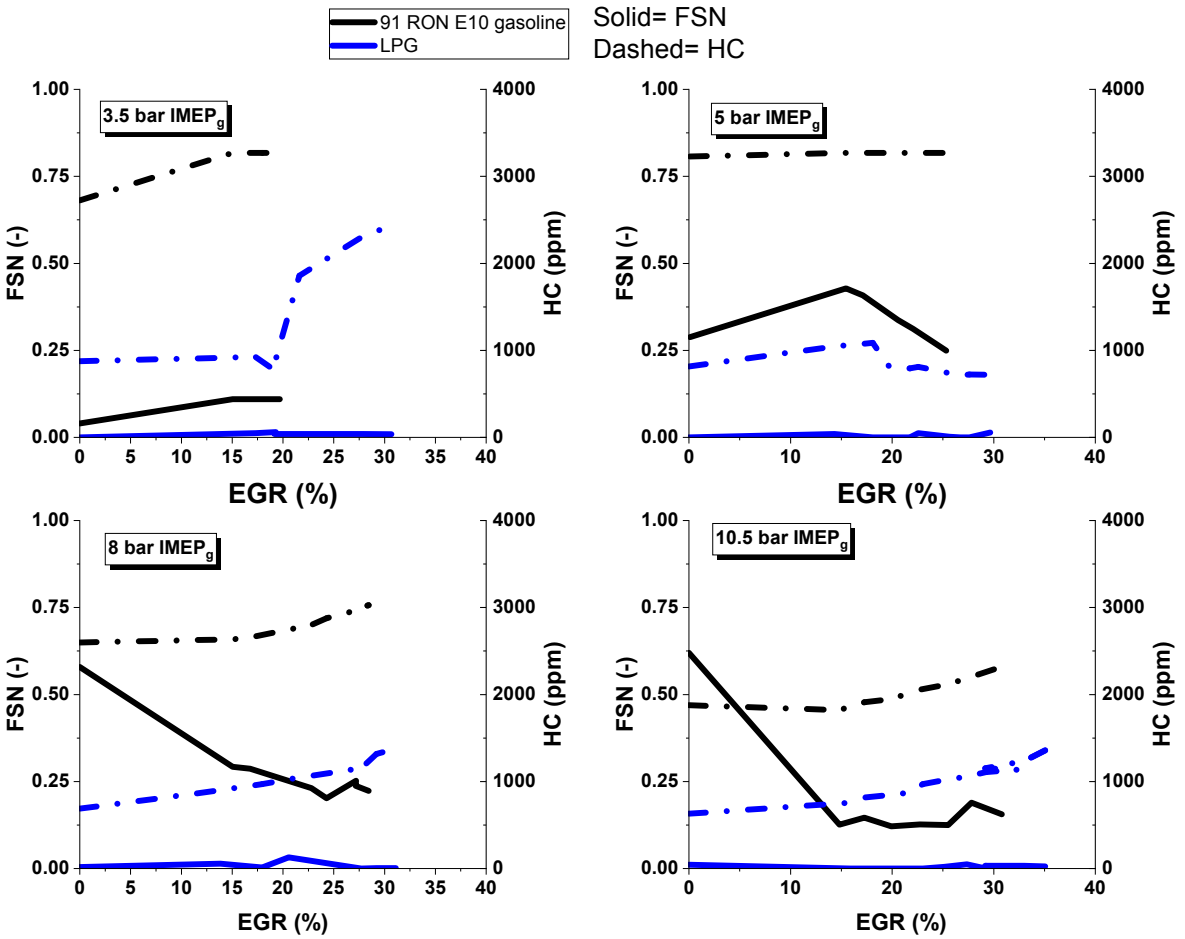

Figure 7. FSN for DI gasoline (black) and LPG (blue) at four loads as a function of EGR at 2000 r/min.

To further analyze the particle emissions from DI LPG compared to gasoline, particle size distributions, and micro soot sensor (MSS) measurements were made. The results for a 0% EGR load sweep are plotted in Figure 8. Results show that like the EGR sweep (Figure 7), LPG has effectively zero FSN,

but the results in Figure 8 also confirm that there is effectively zero soot for LPG as measured with a MSS. Likewise gasoline displayed similar trends in FSN and MSS measurements, which were low, but not an unmeasurable like those of LPG. Simultaneous acquisition of FSN, MSS< and SMPS particle measurements were made. The SMPS results for select loads are plotted in Figure 9, but the total particle number for the load sweep is displayed in Figure 8. Since measurements were conducted on a single cylinder engine, the total particle number (PN) was calculated on an IMEPn basis and corrected for dilution ratio. An average of 3 particle size measurements were made, where the dilution and load normalized average is plotted in Figure 8.

Interestingly despite the differences in soot and FSN between gasoline and LPG, the fuels have total PN that are of the same order and trend relatively well together. Gasoline operation at 13 and 15 bar IMEP was not possible due to knock limit of the fuel, but LPG displays a very interesting trend at these higher loads. Specifically, the total PN count is reduced by an order of magnitude. It is thus hypothesized that most of the particles in both this engine for DI gasoline and LPG are occurring primarily from sources outside those of the fuels themselves, which could be lubricant or valve leakage past exhaust valve seals from the hydraulic Sturman valve system. The sources of these are not directly known but elevated in-cylinder temperatures associated with higher engine loads could be responsible for at least part of the observed total PN reductions. Of particular note is that there is virtually no soot detected by the MSS for LPG whereas even the E85 resulted in measurable

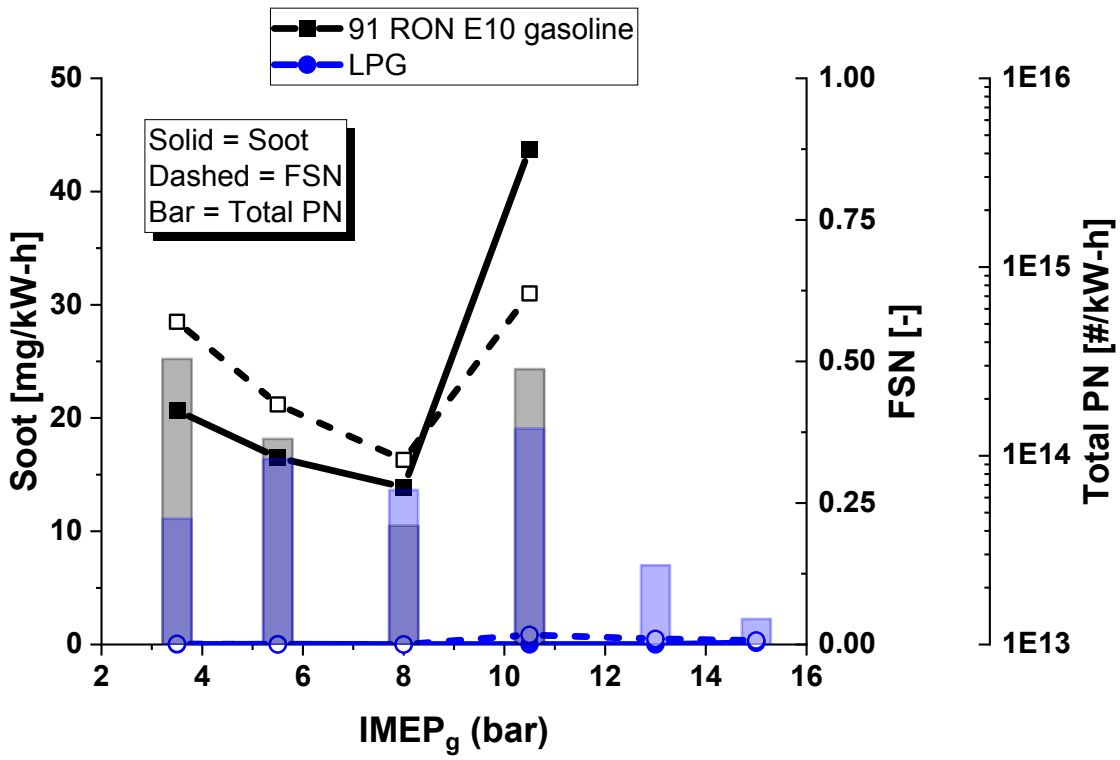

FSN in Szybist et al. [30] despite having lower particle numbers than the observed LPG results here. The lack of soot with LPG here is consistent with the idea that the particles observed with the SMPS are not soot carbon, but lubricant derived aerosols.

Figure 8. Soot, FSN, and total particle number for DI gasoline (black) and LPG (blue) as a function of load at 2000 r/min with 0% EGR.

To further understand the sources of PM in the LPG engine the particle size distributions (PSD) are plotted in Figure 9. The shapes of the PSD of LPG compared to gasoline differ most when the particles are over approximately 100 nm diameter, with more of a pronounced log-normal distribution for the gasoline as compared to LPG. Unlike liquid fuels, the gaseous fuel is not likely to impinge on

the walls or piston and result in pool fires or other sources of combustion particles, so the source of the particles is likely the lubricant and has more to do with the mechanics and temperature of lubricant aerosolization.

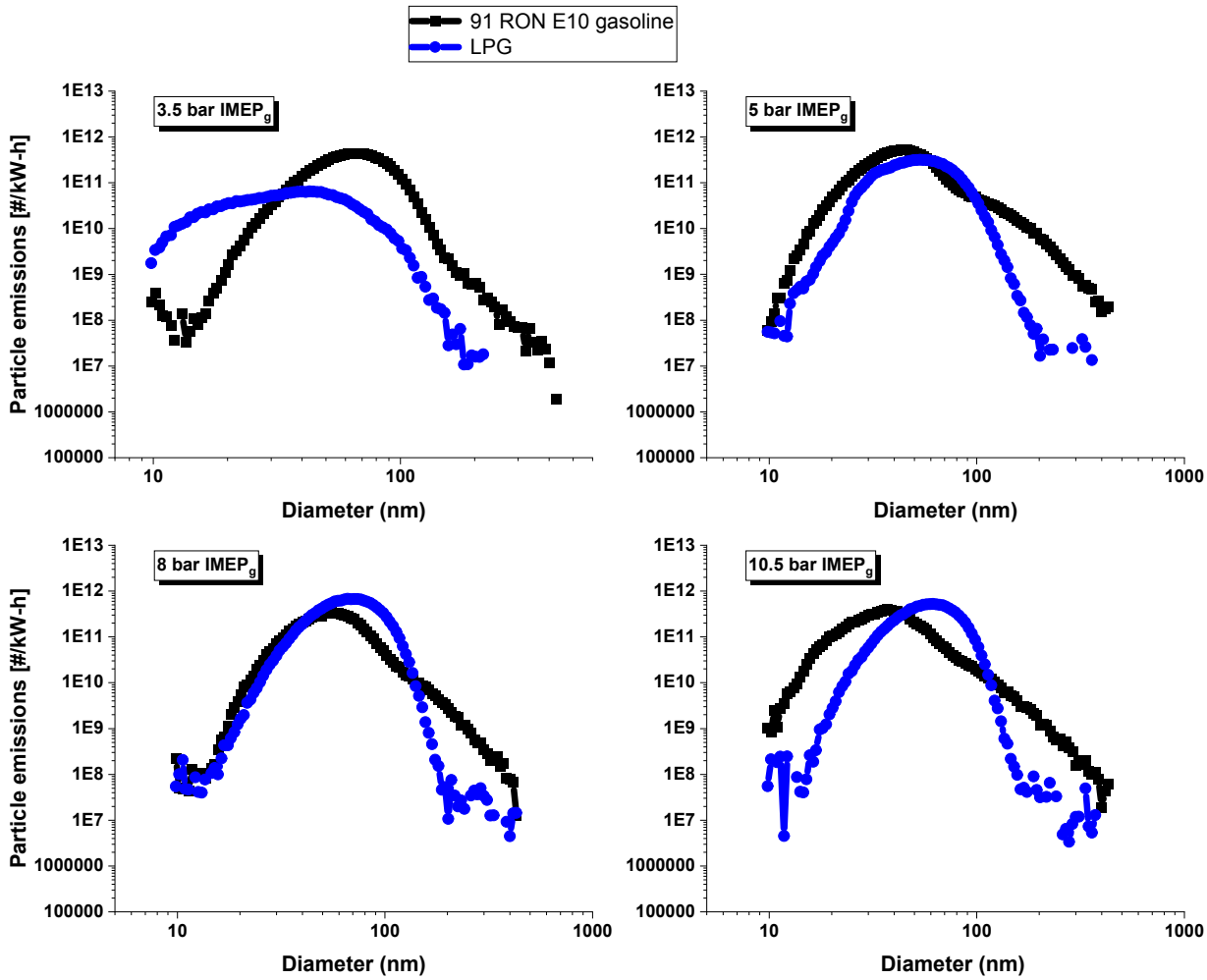

Figure 9. Particle size distributions for DI gasoline (black) and LPG (blue) for four loads at 2000 r/min with 0% EGR.

Consistent with this of lubricant as the primary source of LPG particles, the shapes of the PSD for the propane engine are plotted as a function of load with 0% and 15% EGR in Figure 10, where engine load is observed to reduce the particle size and total number. This is even more pronounced with 15% EGR, which is consistent with literature studies by others [33,34]. In contrast, broad particle size distributions are characteristic of DISI gasoline engines [35,36,37,38]. are not evident with LPG, suggesting that accumulation modes in general are very much reduced. Figure 10 illustrates that accumulation mode particles decay with load, where loads over ~10 bar IMEP show very limited accumulation mode particles (i.e., particles larger than ~30nm) with LPG. These findings combined with the efficiency results of Figure 6 suggest that DI LPG could be a viable opportunity for low emissions high efficiency engines like diesel engines that are common in medium duty applications.

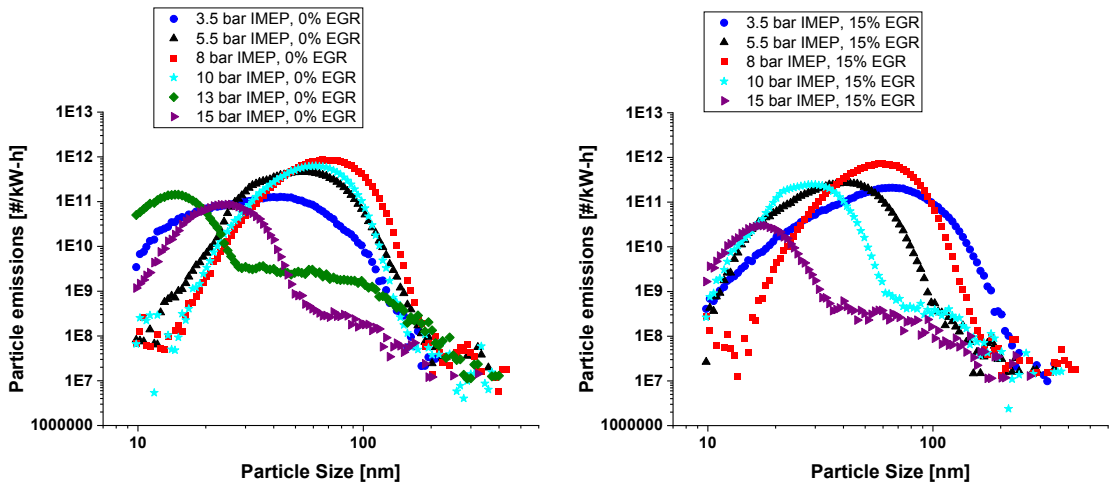

Figure 10. Particle size distributions for LPG load sweeps with (A.) 0% EGR and (B.) 15% EGR

4. Discussion

The present results highlight that low PM and diesel like efficiencies are possible with DI LPG in a high r_c approach. The significance of this is directly applicable to the medium duty engine sector, which, in the United States, is primarily fueled by diesel and gasoline engines. In this sector it is common for 6-7L gasoline and diesel engines to be employed for a wide range of applications. One of the most prevalent engines is the Cummins ISB 6.7L diesel engine. The current results are demonstrated on a 0.75L single cylinder engine, and thus in a V8 configuration this would translate to a 6L total displacement design, which is highly relevant to the United States medium-duty sector.

Therefore, it is of interest to estimate what efficiency and performance of a LSE based LPG engine could be. Efficiency and load were corrected for friction using the default constants used in GT-power as explained in Boronat et al. [14] and Splitter et al. [17, 18]. Because the exact friction is unknown, the friction was estimated not as a direct number but a range. It was assumed that technologies to reduce friction could be applied to reduce friction up to 40% over default GT-Power values, which is relevant to what literature values have been reported by others [40]. The results of this analysis with the best efficiency LSE LPG results are plotted in Figure 11 and compared to the NHSTA reported values of the 2019 Cummins ISB, which are used for certification purposes. Clearly the results of DI LPG very closely approach those of the ISB in terms of brake thermal efficiency (BTE) and output (BMEP). Note that the load sweep with the LPG engine was prematurely stopped because the fuel injection system was unaltered form the stock engine and the injector duration needed for high load was beyond the safety limits imposed by the control software. A LPG specific injector design with increased flowrate would likely be required for further load expansion demonstration.

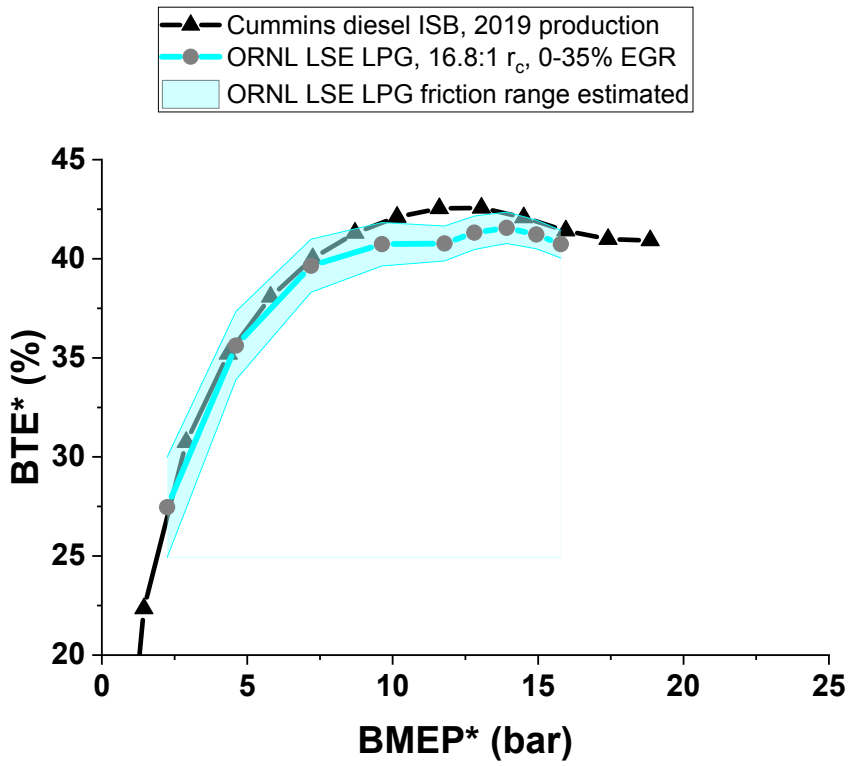

Figure 11. ORNL LSE derived BTE numbers compared to 2019 production Cummins ISB diesel.

The ramifications of the efficiency illustrated in Figure 11 become apparent when examined form the perspective of pending 2027 emissions and efficiency regulation in the United states, which will regulate CO2 emissions in medium duty vehicles. Specifically, the 2027 standards are 457 [gCO_2/bhp-hr] and 535 [gCO_2/bhp-hr] in the SET cycle and FTP cycles respectively [39]. Since the emissions regulations are on a vehicle CO2 basis and not a, efficiency basis there are great potential opportunities for reduced carbon intensity fuels like LPG.

According to a national LPG survey by the Propane Education and Research Council (PERC) from 2017 and 2018 [41], LPG is between 91–96% on average propane, with the balance species of ethane (0.5–6.5%) and combinations of butane and its isomers (up to 7.5%). The significantly increased H/C ratio of LPG ~2.67:1 is attractive for reducing CO_2 emissions by ~12% (energy basis when compared with diesel fuel) in a stoichiometric SI engine if engine brake thermal efficiency (BTE) parity with diesel is achieved, presenting a pathway to beyond 2027 compliance.

The results in the present work and that of Boronat et al. [14] illustrate that an engine design that exploits LPG's unique properties, greatly improves efficiency, and enables significantly higher r_c is possible. As shown in Boronat et al. [14], and Figure 6 and Figure 11 of the present work, diesel engine efficiency parity to the 2019 Cummins ISB is possible. Similar work has been conducted by Rengarajan et al. [42], in a multi cylinder engine but with lower efficiency than the present work due to reduced compression ratio and reduced stroke-to-bore ratio. The 2019 ISB is certified at 488 [gCO_2/bhp-hr] (SET steady-state) and 525 [gCO_2/bhp-hr] (FTP transient) [43], translating to 40.7% SET and 37.8% FTP cycle-averaged efficiency.

The present work highlights proof-of-concept results as illustrated in Figure 11 that DI LPG can approach or meet the Cummins 2019 ISB efficiencies. Thus, a similar SET and FTP transient efficiency to the ISB might be possible with DI LPG using an approach like the LSE. With further optimization and development, a target of 41% SET average with DI-LPG might be possible while meeting all applicable 2027 criteria emissions regulations as three-way catalyst of this program is highly possible as highlighted by previous work by others [44]. Achieving the such a cycle efficiency with LPG would result in cycle CO_2 emissions of 430gCO_2/hp.hr, a 6% reduction from 2027 Phase 2 greenhouse gas (GHG) regulations and illustrate a pathway for SI engine approaches to meet or exceed 2027 emission regulation using DI LPG.

5. Conclusions

The present work illustrated performance and emissions of DI LPG and gasoline in a novel lone stroke engine (LSE). The major findings of the present work are outlined as the following.

1. Regardless of liquid petroleum gas (LPG) or gasoline fueling the LSE engine exhibited significantly improved combustion durations, which were ~20% faster than the production GM LNF engine, when using the same piston and TDC geometry. When using the similar compression ratios (i.e. a "dome" piston in the LNF was required), the LSE exhibited even further combustion duration benefits. These differences were attributed to significantly increased turbulence from the LSE's increase stroke
2. With gasoline the LSE was found to offer significantly improved HC and combustion efficiency improvements when high compression ratio was used. This was again attributed to the combustion chamber improvment for a given compression ratio with the LSE compared to the LNF. However, with DI LPG the advantages were reduced as HC emissions were extremely low with LPG overall.
3. LPG was found to enable increased EGR rate compared to gasoline (20-50% relative increase depending on load). The results were attributed to fundamental flame dynamics and combustion properties such as flame stretch differences of LPG vs. gasoline when EGR is used.
4. A combination of DI LPG with LIVC (110°CA $bTDC_f$), EGR (~30%) and high r_c (16.8:1) was found to yield in excess of 45% NTE with diesel like power density. This was an improvement of ~30% relative to the production engine with DI LPG.
5. DI LPG was found to have effectively zero measurable FSN and soot, but similar PN to gasoline. Particle size distribution (PSD) as a function of load showed that as load increased regardless of 0% or 15% EGR, DI LPG exhibited smaller diameter and lower number counts of particles. This translated to reductions in total PN overall. These combined results were postulated to be an effect of significantly reduced wall wetting with DI LPG as compared to gasoline.
6. Efficiency results were compared to a conventional MD diesel engine in the form of the 2019 Cummins ISB. Brake thermal efficiency of the single-cylinder LSE was estimated by a friction correlation and compared very favorably to the efficiency of the Cummins engine and power density. The results show promise for pathways of low GHG/CO2 fuels to meet future emissions regulation with SI TWC compatible combustion.

6. Contact

Derek Splitter
splitterda@ornl.gov

5. Acknowledgements

This research was supported by the DOE Office of Energy Efficiency and Renewable Energy (EERE), Vehicle Technologies Office and used resources at the National Transportation Research Center, a DOE-EERE User Facility at Oak Ridge National Laboratory. A special thanks to DOE program managers Kevin Stork, Michael Weismiller, and Gurpreet Singh for funding this work.

7. References

1. Wissink, M.L., Splitter, D.A., Dempsey, A.B., Curran, S.J., Kaul, B.C. and Szybist, J.P., 2017. An assessment of thermodynamic merits for current and potential future engine operating strategies. *International Journal of Engine Research*, *18*(1-2), pp.155-169.
2. Alger, T., Mangold, B., Roberts, C. and Gingrich, J., 2012. The interaction of fuel anti-knock index and cooled EGR on engine performance and efficiency. *SAE International Journal of Engines*, *5*(3), pp.1229-1241.
3. Szybist, J.P., Wagnon, S.W., Splitter, D., Pitz, W.J. and Mehl, M., 2017. The reduced effectiveness of EGR to mitigate knock at high loads in boosted SI engines. *SAE International Journal of Engines*, *10*(5), pp.2305-2318.

4. Szybist, J.P., Youngquist, A.D., Barone, T.L., Storey, J.M., Moore, W.R., Foster, M. and Confer, K., 2011. Ethanol blends and engine operating strategy effects on light-duty spark-ignition engine particle emissions. *Energy & Fuels*, *25*(11), pp.4977-4985.
5. Jatana, G.S., Splitter, D.A., Kaul, B. and Szybist, J.P., 2018. Fuel property effects on low-speed pre-ignition. *Fuel*, *230*, pp.474-482.
6. Chapman, E.; Davis, R.; Studzinski, W.; Geng, P. (2014). "Fuel Octane and Volatility Effects on the Stochastic Pre-Ignition Behavior of a 2.0L Gasoline Turbocharged DI Engine". *SAE Int. J. Fuels Lubr*. **7** (2): 379–389. doi:10.4271/2014-01-1226.
7. Craig, A., Warkins, J., Aravelli, K., Moser, D. et al., "Low Cost LEV-III, Tier-III Emission Solutions with Particulate Control using Advanced Catalysts and Substrates," *SAE Int. J. Engines* 9(2):1276-1288, 2016, https://doi.org/10.4271/2016-01-0925.
8. Johnson, T., "Vehicular Emissions in Review," *SAE Int. J. Engines* 9(2):1258-1275, 2016, https://doi.org/10.4271/2016-01-0919.
9. CARB "California Air Resources Board Staff Current Assessment of the Technical Feasibility of Lower NOx Standards Associated Test Procedures for 2022 and Subsequent Model Year Medium-Duty and Heavy-Duty Diesel Engines", accessed 02/20/2020.
10. Posada, F., Badshah, H., Rodriguez, F. (2020). In-use NOx emissions and compliance evaluation for modern heavy-duty vehicles in Europe and the United States. Retrieved from The International Council on Clean Transportation website: https://theicct.org/publications/inuse-nox-hdvs-us-eu, accessed 06/01/2020.
11. Neely, G., Sharp, C., and Rao, S., "CARB Low NOx Stage 3 Program - Modified Engine Calibration and Hardware Evaluations," SAE Technical Paper 2020-01-0318, 2020, https://doi.org/10.4271/2020-01-0318.
12. Rao, S., Sarlashkar, J., Rengarajan, S., Sharp, C. et al., "A Controls Overview on Achieving Ultra-Low NOx," SAE Technical Paper 2020-01-1404, 2020, https://doi.org/10.4271/2020-01-1404.
13. Dieselnet, "United States: Heavy-Duty Vehicles: GHG Emissions & Fuel Economy", accessed 02/20/2020, https://dieselnet.com/standards/us/fe_hd.php#co2
14. Boronat, V., Splitter, D., and Dal Forno Chuahy, F., "Achieving Diesel-Like Efficiency in a High Stroke-to-Bore Ratio DISI Engine under Stoichiometric Operation," SAE Technical Paper 2020-01-0293, 2020, doi:10.4271/2020-01-0293.
15. Szybist, J.; Foster, M.; Moore, W.; Confer, K. Investigation of Knock Limited Compression Ratio of Ethanol Gasoline Blends. SAE Technical Paper 2010-01-0619; 2010; DOI: 10.4271/2010-01-0619.
16. Splitter, D.A. and Szybist, J.P., 2014. Experimental investigation of spark-ignited combustion with high-octane biofuels and EGR. 2. Fuel and EGR effects on knock-limited load and speed. *Energy & Fuels*, *28*(2), pp.1432-1445.
17. Splitter, D.A. and Szybist, J.P., 2014. Experimental investigation of spark-ignited combustion with high-octane biofuels and EGR. 1. Engine load range and downsize downspeed opportunity. *Energy & Fuels*, *28*(2), pp.1418-1431.
18. Splitter, D. and Szybist, J., 2014. Intermediate alcohol-gasoline blends, fuels for enabling increased engine efficiency and powertrain possibilities. *SAE International Journal of Fuels and Lubricants*, *7*(1), pp.29-47.
19. Cavina, N., Siviero, C., Suglia, R., "Residual Gas Fraction Estimation: Application to a GDI Engine with Variable Timing and EGR". SAE Int Engines. 2004-01-2943.
20. Woschni, G., " A Universally Applicable Equation for the Instantaneous Heat Transfer Coefficient in the Internal Combustion Engine," SAE Transactions, Vol. 76, 1967, p. 3065.
21. Gatowski, J. A., En N. Balles, Kwang Min Chun, F. E. Nelson, J. A. Ekchian, and John B. Heywood. "Heat release analysis of engine pressure data." SAE transactions (1984): 961-977.
22. Tunestål, Per. "TDC offset estimation from motored cylinder pressure data based on heat release shaping." Oil & Gas Science and Technology–Revue d'IFP Energies nouvelles 66, no. 4 (2011): 705-716.
23. Caris, D. F., and E. E. Nelson. "a new look at High Compression Engines". No. 590015. SAE Technical Paper, 1959. https://doi.org/10.4271/590015
24. Peters, N. (1999). The turbulent burning velocity for large-scale and small-scale turbulence. Journal of Fluid Mechanics, 384, 107-132
25. Enaux, B., et al. (2011). "LES study of cycle-to-cycle variations in a spark ignition engine." Proceedings of the Combustion Institute 33(2): 3115-3122.

26. Zhao, L., et al. (2017). "Examining the role of flame topologies and in-cylinder flow fields on cyclic variability in spark-ignited engines using large-eddy simulation." International Journal of Engine Research 19(8): 886-904.
27. Mounaïm-Rousselle, C., et al. (2013). "Experimental characteristics of turbulent premixed flame in a boosted Spark-Ignition engine." Proceedings of the Combustion Institute 34(2): 2941-2949.
28. T. Kitagawa, Y. Togami, K. Harada, T. Ogawa, Effects of Pressure on Unstretched Laminar Burning Velocity, Markstein Length and Cellularity of Propagating Spherical Laminar Flames, Transactions of the Japan Society of Mechanical Engineers Series B 70 (2004) 2197-2204.
29. B. Galmiche, F. Halter, F. Foucher, Effects of high pressure, high temperature and dilution on laminar burning velocities and Markstein lengths of iso-octane/air mixtures, Combustion and Flame 159 (2012) 3286-3299.
30. Szybist, J.P., Youngquist, A.D., Barone, T.L., Storey, J.M., Moore, W.R., Foster, M. and Confer, K., 2011. Ethanol blends and engine operating strategy effects on light-duty spark-ignition engine particle emissions. *Energy & Fuels*, *25*(11), pp.4977-4985.
31. Moore, W.; Foster, M.; Lai, M.-C.; Xie, X.-B.; Zheng, Y.; Matsumoto, A. Charge motion benefits of valve deactivation to reduce fuel consumption and emissions in a GDi, VVA engine. SAE [Tech. Pap.] 2011, DOI: 10.4271/2011-01-1221.
32. Sabathil, D.; Koenigstein, A.; Schaffner, P.; Fritzsche, J.; Doehler, A. The influence of DISI engine operating parameters on particle number emissions. SAE [Tech. Pap.] 2011, DOI: 10.4271/2011-01-0143.
33. Alger, T., Gingrich, J., Khalek, I.A. and Mangold, B., 2010. The role of EGR in PM emissions from gasoline engines. *SAE International Journal of Fuels and Lubricants*, *3*(1), pp.85-98.
34. Zhang, Z., Wang, T., Jia, M., Wei, Q., Meng, X. and Shu, G., 2014. Combustion and particle number emissions of a direct injection spark ignition engine operating on ethanol/gasoline and n-butanol/gasoline blends with exhaust gas recirculation. *Fuel*, *130*, pp.177-188.
35. Storey, JME, Lewis, SA, Szybist, JP., Thomas, JF., Barone, T.L., Eibl, MA, and Kaul, B, “Novel Characterization of GDI Engine Exhaust for Gasoline and Mid-Level Gasoline-Alcohol Blends,” SAE Int. J. Fuels Lubr., vol. 7, pp. 1-8, 2014.
36. Storey, JME, TL Barone, JF Thomas, and SP. Huff, 2012. “Exhaust Particle Characterization for Lean and Stoichiometric DI Vehicles Operating on Ethanol-Gasoline Blends,” SAE Technical Paper Series 2012-01-0437, 2012.
37. Barone, TL, JME Storey, AD Youngquist, and JP Szybist. 2012. "An analysis of direct-injection spark-ignition (DISI) soot morphology," Atmospheric Environment 49, 268-274.
38. Koczak, J., Boehman, A., and Brusstar, M., "Particulate Emissions in GDI Vehicle Transients: An Examination of FTP, HWFET, and US06 Measurements," SAE Technical Paper 2016-01-0992, 2016, https://doi.org/10.4271/2016-01-0992.
39. Dieselnet, “United States: Heavy-Duty Vehicles: GHG Emissions & Fuel Economy”, accessed 02/20/2020, https://dieselnet.com/standards/us/fe_hd.php#co2
40. Delgado, O. and Lutsey, N., 2014. The US SuperTruck Program. Washington DC.
41. Reinhart, T.E., 2015. Commercial medium-and heavy-duty truck fuel efficiency technology study-Report# 1 (No. DOT HS 812 146).
42. Rengarajan, S., Liu, Z., Lerin, C., Stetter, J., Narang, V. and Lana, C., 2020. LPG Direct Injection Engine for Medium Duty Trucks (No. 2020-01-5008). SAE Technical Paper.
43. EPA, “Annual Certification Data Vehicles, Engines and Equipment”, accessed 04/24/2020, https://www.epa.gov/compliance-and-fuel-economy-data/annual-certification-data-vehicles-engines-and-equipment
44. Zigler, Bradley T, Toops, Todd, Krishnan, Sundar, and Srinivasan, Kal-yan. Direct Injection 4.3 L Propane Engine Research, Development, and Test-ing. United States: N. p., 2019. https://www.nrel.gov/docs/fy19osti/73876.pdf